ACS APPLIED MATERIALS & INTERFACES

Research Article

www.acsami.org

Self-Driven One-Step Oil Removal from Oil Spill on Water via Selective-Wettability Steel Mesh

Jinlong Song,[†,‡] Shuai Huang,[‡] Yao Lu,[§] Xiangwei Bu,[‡] Joseph E. Mates,[†] Aritra Ghosh,[†] Ranjan Ganguly,[†,∥] Claire J. Carmalt,[§] Ivan P. Parkin,[§] Wenji Xu,*[,‡] and Constantine M. Megaridis*[,†]

[†]Department of Mechanical and Industrial Engineering, University of Illinois at Chicago, Chicago, Illinois 60607, United States

[‡]Key Laboratory for Precision and Non-traditional Machining Technology of Ministry of Education, Dalian University of Technology, Dalian 116024, China

[§]Materials Chemistry Research Centre, Department of Chemistry, University College London, 20 Gordon Street, London WC1H OAJ, U.K.

[∥]Department of Power Engineering, Jadavpur University, Kolkata 700098, India

Supporting Information

ABSTRACT: Marine oil spills seriously endanger sea ecosystems and coastal environments, resulting in a loss of energy resources. Environmental and economic demands emphasize the need for new methods of effectively separating oil–water mixtures, while collecting oil content at the same time. A new surface-tension-driven, gravity-assisted, one-step, oil–water separation method is presented for sustained filtration and collection of oil from a floating spill. A benchtop prototype oil collection device uses selective-wettability (superhydrophobic and superoleophilic) stainless steel mesh that attracts the floating oil, simultaneously separating it from water and collecting it in a container, requiring no preseparation pumping or pouring. The collection efficiencies for oils with wide ranging kinematic viscosities (0.32–70.4 cSt at 40 °C) are above 94%, including motor oil and heavy mineral oil. The prototype device showed high stability and functionality over repeated use, and can be easily scaled for efficient cleanup of large oil spills on seawater. In addition, a brief consolidation of separation requirements for oil–water mixtures of various oil densities is presented to demonstrate the versatility of the material system developed herein.

KEYWORDS: *oil/water separation, oil spill cleanup, self-driven separation, wettability, stainless steel mesh*

1. INTRODUCTION

Oil spills resulting from oil exploration, transportation, and storage pose great environmental risk; a durable, scalable solution is required to mediate damage from future accidents, as present cleanup methods are far from adequate. The risk of oil spills underscores the need to develop simple, yet effective, techniques for efficient separation and removal of oil from the spill site. In the case of large-scale oil spills on water, besides the immediate threat to marine species and their ecosystem, the natural and economic ramifications of the disaster may last for more than a decade after the event. Oil containment booms are often used to stop oil dispersal prior to disposal.[1] For thick oil spill top-layers, the oil can be collected by oil skimmers or simply be burnt out. However, most skimmers are inefficient, required in large numbers, and leave much of the recovered oil mixed with water.[2] Likewise, in situ combustion is only partially successful, creates toxic fumes, and stops being effective when the floating oil layer thins. For "thin-spills," oil-absorbent materials are commonly used. The most prevalent commercial oil-absorption materials are polypropylene-based felts. These materials have several drawbacks, which include inadequate absorption capacity, low selectivity, and poor recyclability. Other oil-absorbing materials, for example, zeolites, activated carbon, organoclays, straw, hair, and wool fibers also have similar limitations.[3−5] Apart from the aforementioned methods, dispersants and oil consuming microbes are also deployed to clean oil spills.[6,7] However, expensive dispersants are often toxic, and the dispersed oil resulting from this method can settle and pollute the ocean floor. Oil-eating microbes also pose problems in large numbers, as they can reduce subsea oxygen levels, thereby threatening marine life and the delicate balance of the surrounding ecosystem.[2] Therefore, the development of new oil/water separation methods with high efficiency, low cost and improved safety has been the focus of extensive research in this area.

Recently, materials with special wettabilities and micro/nanometer-scale structures have attracted increased attention for oil/water separation.[8,9] Extreme wettability properties (e.g.,

Received: August 5, 2014
Accepted: October 20, 2014
Published: October 20, 2014

superhydrophobicity, superhydrophilicity, superoleophobicity, or superoleophilicity) can be attained by adjusting surface micro/nanostructures and surface energy.[10−15] To resolve the drawbacks of the prevailing oil/water separation methods, materials that simultaneously display superhydrophobic−superoleophilic or superhydrophilic−superoleophobic properties have been studied as a means to separate oil and water. The methods developed for oil spill cleanup based on new materials can be classified in two main categories. The first, uses oil absorbent materials, such as superhydrophobic−superoleophilic textiles,[16−19] polymer sponges,[20−23] metal sponges,[24,25] paper,[26] carbon nanotube sponges,[27] nanocellulose aerogels,[28,29] or macroporous gels.[30] These materials can absorb oil while simultaneously repelling water, often exhibiting high oil/water separation efficiency and selectivity. However, retrieving the oil requires mechanical handling (squeezing/compression) after each absorption cycle, which is cumbersome for continuous separation in large-area oil spills. The second approach for oil spill cleanup employs oil or water filtration materials, such as superhydrophobic−superoleophilic or superhydrophilic−superoleophilic (underwater superoleophobic) meshes (metal, polymer, or fabric-based), which are usually referred to as "oil-removing" or "water-removing" materials; these meshes selectively let either oil or water pass through them, thus facilitating separation of the two immiscible liquids.[31−39] The oil or water filtration materials in other studies have mostly been combined with pouring-type, gravity-driven procedures to realize oil/water separation.

The pioneering work of Feng et al., wherein a steel mesh was spray-coated with an extremely durable polymer composite, was one of the first to report the utility of superhydrophobic/superoleophilic durable substrates in selective separation of oil and water using pouring-type, gravity-driven approaches.[31] Variants of this technology using mesh filters have been extensively studied in an effort to create more efficient, durable, and relatively inexpensive routes to mitigate the disastrous effects of oil spills on water. Tuteja and co-workers used this concept to develop an elegant pouring method that harnessed gravity as the only force required for separating oil/water mixtures and collecting the oil.[32] However, oil or water filtration based on traditional pouring-type gravity-driven methodologies requires the oil/water mixture to be collected in bulk first, and then poured onto the mesh.[31−39] This approach can be cumbersome and energy-intensive for large-area oil spills. Therefore, it is important to develop direct methods that do not require a pouring step. Additionally, pouring-type gravity-driven separation studies reported in the literature have been demonstrated with a variety of immiscible fluids without a logical consolidation of conditions. Some researchers have opted to demonstrate separation from water using light oils ($\rho_{oil} < \rho_{water}$),[31,37] while others have chosen heavy oils ($\rho_{oil} > \rho_{water}$) for similar experiments.[38,39] Consequently, there exists a need in the literature for defining all demonstrable modes of separation, whether gravity- or self-driven.

Stainless steel meshes are often selected by researchers for oil or water filtration/separation because of their superior physical, chemical, and mechanical properties, wide availability, and relatively low cost. Several methods, including spray-dry,[31] hydrogel-coating,[33,40] silica sol-coating,[41] seed-growth,[42,43] magnetron sputtering,[44] electrochemical deposition,[45] and layer-by-layer assembly methods,[36] have been developed to fabricate superhydrophobic or superhydrophilic stainless steel meshes, which were subsequently used to separate oil/water mixtures. Most of these fabrication methods have drawbacks with regards to their economically viable, large-scale implementation, as they require either high-temperature treatment,[31] UV irradiation,[33] cyclic dipping,[36] or gel synthesis,[40,41] complex or expensive equipment (e.g., programmable dipping robot,[36] magnetron sputterer,[44] or electrochemical instrumentation[45]), or relatively long processing times (over 12 h[40−44]). Worse yet, some coatings can easily be stripped off after several cycles of separation and do not offer the durability needed for real-world applications.[33,46]

The present study describes a facile method to fabricate superhydrophobic stainless steel meshes for novel, pumpless, one-step, in situ oil/water separation; the method is scalable and thus appropriate for large-area application. The method relies on surface tension-driven, gravity-assisted principles, and the corresponding oil filtration mass flux can be readily quantified. This filtering method allows sustained on-site separation of oil/water mixtures without prior collection, lifting or pouring of the mixture, thus ridding the requirement of any pump or power input for removing the oil from the spill site. Simultaneous filtration of oil/water mixtures and oil collection are demonstrated using this filter device, with high oil/water separation efficiency, leading to nearly complete oil collection, in some cases at rates of several kg/s·m^2. Interestingly, the adhered/adsorbed oil in the deployed mesh filters does not affect separation; separation efficiencies exceeding 92% are retained even after 58 repeated use cycles, a relatively small decline from their peak performance of greater than 95% efficiency. Flow visualization confirms that the superhydrophobic mesh allows sustainable bulk flow of oil through it while blocking water flow. The fabrication technique is easily scaled with potential for automation in open-sea applications, making it an attractive option for low-cost and effective oil spill cleanup.

2. EXPERIMENTAL SECTION

2.1. Preparation of Superhydrophobic Meshes. The stainless steel meshes (type 201) were initially cleaned by detergent and deionized water. After drying, the meshes were immersed in an aqueous solution of 1 M $CuCl_2$ and 1 M HCl at room temperature for different time durations (1, 2, 4, 7, 11, 16, and 22 s). After their timed exposure, the meshes were removed from the bath and rinsed again using deionized water. The resulting meshes turned red from their original silvery white color and showed hydrophilic or superhydrophilic properties (depending on the duration of immersion). Then, the freshly prepared, dry meshes were immersed in a 0.05 mol/L ethanol solution of stearic acid for 20 min and then dried using a standard air drier. The stearic acid-modified meshes showed hydrophobic or superhydrophobic properties. It is important to note that the present method is limited only in terms of immersion container size and could easily be scaled for larger mesh sizes and thus larger collection vessels. The immersion process could even be added inline to an industrial manufacturing process with potential for high throughput roll-to-roll production.

2.2. Characterization. The morphologies of the samples were characterized using a scanning electron microscope (SEM, JSM−6360LV, Japan). Mesh chemical composition was characterized using an X-ray diffractometer (Empyrean, Holland) and energy-dispersive X-ray analysis (EDS, INCA Energy, Oxford Instruments). The purity of the separated oil was quantified using differential scanning calorimetry (DSC, Q200, TA Instruments). Control samples of known proportions of hexadecane and water mixtures were heated through the boiling point of water; the change in heat capacity (ΔC_p) of the control mixtures was then compared against that of pure water under the same conditions. Oil/water mass ratios based on ΔC_p changes were confirmed to within the 0.9% accuracy of the DSC and the

Table 1. Oil Properties

oil	hexane (Sigma-Aldrich, #178918)	hexadecane (Sigma-Aldrich, #H6703)	motor oil (Orbit Oil, SAE 5−30)	heavy mineral oil (Sigma-Aldrich, #330760)	chloroform (Sigma-Aldrich #319988)
density at 25 °C [g/cm^3]	0.65	0.77	0.85	0.86	1.48
surface tension at 20 °C [mN/m]	17.9	27.5	40.1 ± 0.5[a]	28.5	27.1
kinematic viscosity at 40 °C [cSt]	0.42	2.9	60.1	63.6−70.4	0.32

[a]Surface tension measured using the pendant droplet method.

preweighed (Sartorius LE26P microbalance) oil/water amounts. Water and oil droplet contact angle and sliding angle measurements were performed using an in-house goniometer employing ∼5 μL water and oil droplets. The sliding angle was defined as the angle at which the liquid drop began to slide on the gradually inclined surface. The oils used in the present study include hexane, hexadecane, motor oil, heavy mineral oil, and chloroform; their relevant properties are summarized in Table 1. Hexadecane and chloroform were dyed with Oil Red O ($C_{26}H_{24}N_4O$) and Oil Blue N ($C_{24}H_{30}N_2O_2$), respectively, for visualization. 0.29 g of poly(tetrafluoroethylene) (PTFE) particle powder (∼1 μm diameter) was added into 14.5 g of hexadecane to form the oil−PTFE dispersion used to demonstrate robust separation even in the presence of fouling contaminants.

Roughness measurements (RMS) were technically difficult on the fine mesh, as the contours of the mesh metal fibers made precision estimates of added roughness delivered by Cu treatment infeasible without damaging the initial micro/nano structures. Alternatively, when attempting to perform comparison measurements on smooth, flat stainless steel sheets, the much lower surface area of the flat sheets changed the efficacy of the chemical reaction and was thus not considered a valid comparison. A more thorough investigation of added roughness via the chemical reactions described herein is planned for a later publication; however, intrinsic to any contact angle measurement is an indirect quantitative roughness measurement, which was considered to be sufficient for presenting this novel technique, and is complementary to the more qualitative SEM verification of roughness as a function of chemical reaction time.

3. RESULTS AND DISCUSSION

Figure 1a−d shows SEM images, at increasing magnifications (from upper to lower rows), of newly prepared stainless steel mesh samples after timed immersion in aqueous solution of 1 M $CuCl_2$ and 1 M HCl (first wet-processing step). The morphology of the emerging mesh was greatly influenced by the immersion time. For the unexposed stainless steel mesh, the wire surfaces were very smooth [Figure 1a]. The average size of the wire diameter and open pores were 53.3 and 73.7 μm, respectively. For an immersion time of 1 s, pointed and plate-shaped protrusions with size ranging from several hundred nanometers to several micrometers were uniformly formed on the surface of the wires [Figure 1b]. Higher immersion times encouraged formation of longer surface features that in some locations resembled leaflike structures. It can be seen from Figure 1c that these leaflike structures grew orthogonally out of the mesh wire walls after only 2 s of immersion. When the immersion time increased to 7 s, the leaflike surface structures were even more prevalent, with many being intertwined with each other [Figure 1d]. The magnified SEM image in the lowermost pane of Figure 1d shows a typical leaf structure with an edge length of ∼10 μm and a width of ∼6 μm. All branches grew sideways from the metal-wire trunk, forming a parallel and periodic array.

Energy dispersive spectrometry (EDS) analysis showed evidence of very strong Cu peaks for the meshes immersed for 7 s (Figure 1f), but not for the unexposed steel meshes

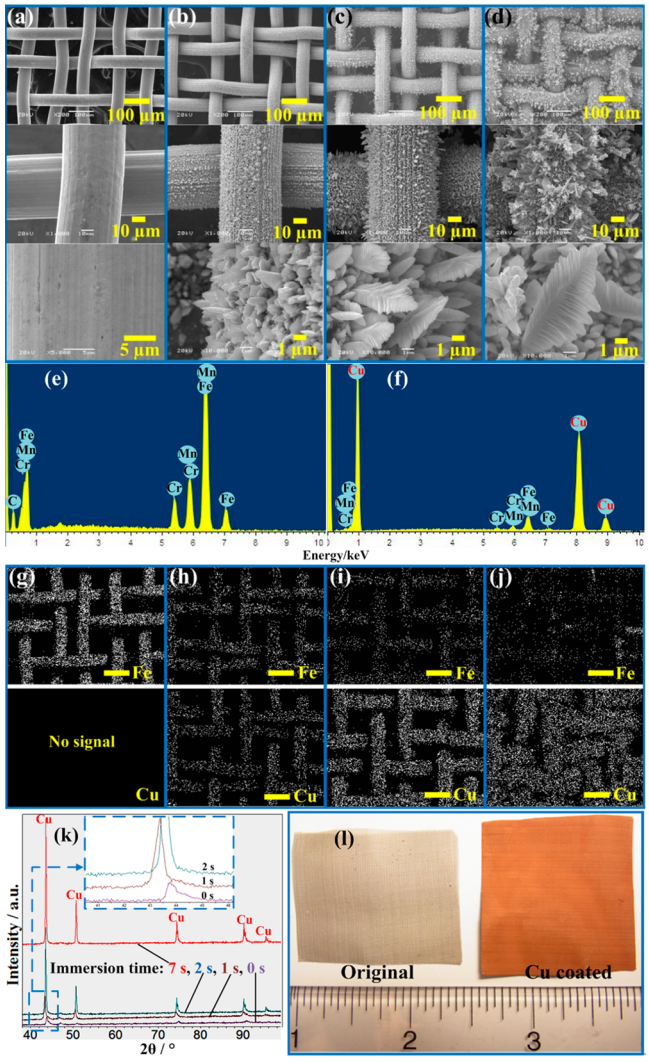

Figure 1. Surface morphology and chemical composition of stainless steel meshes at different immersion times in an aqueous solution of 1 M $CuCl_2$ and 1 M HCl. SEM images of newly prepared mesh samples after immersion times of (a) 0 s, (b) 1 s, (c) 2 s, and (d) 7 s. (e, f) EDS spectra of samples (a, d), respectively. (g, h, i, j) EDS elemental maps of Fe (upper) and Cu (lower) for samples (a, b, c, d), respectively (scale bar is 100 μm for these frames). (k) XRD patterns of samples (a)−(d). (l) Macro-images of the original and Cu-coated stainless steel meshes.

(Figure 1e). In addition, the elemental fraction of Cu increased progressively with immersion time [see Cu maps in bottom row; Figure 1(g−j)]. The opposite trend was seen for iron [see top-row maps; Figure 1(g−j)], as the Fe elemental fraction (in steel) decreased with immersion duration, which increased coverage of the stainless steel mesh by the Cu-containing

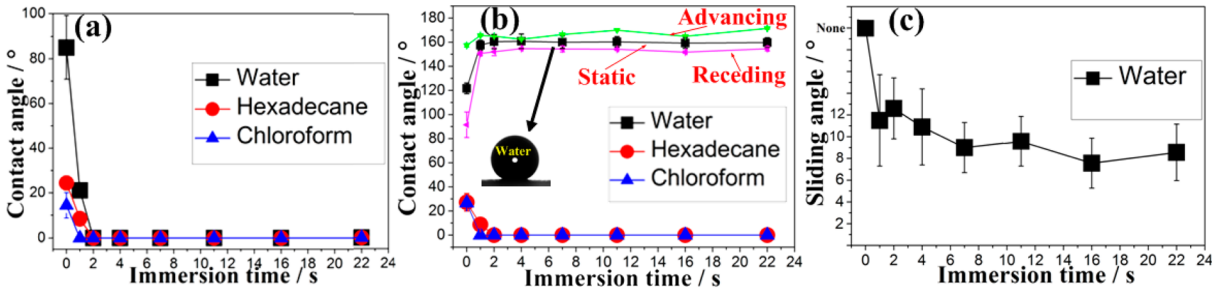

Figure 2. Contact and sliding angles of water, hexadecane, and chloroform droplets on mesh samples in air. The meshes were first immersed for the specified time periods in a $CuCl_2$−HCl solution and subsequently treated in STA. (a) Before 0.05 mol/L STA modification for 20 min; (b, c) after 0.05 mol/L STA modification for 20 min.

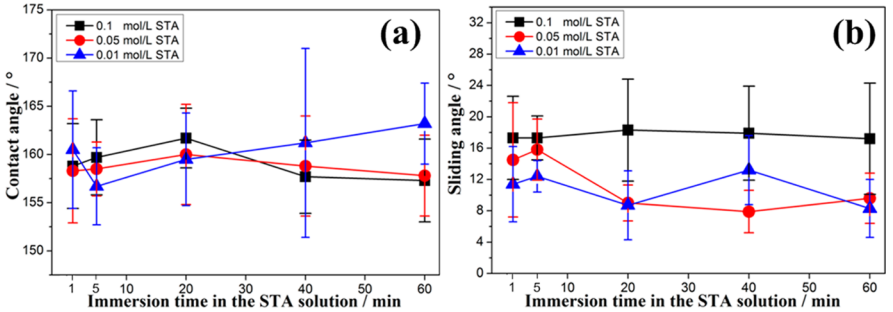

Figure 3. Variation of water contact and sliding angles on mesh with immersion time in the stearic acid (STA) solution at three different concentrations (the micro roughness was produced by immersion in the aqueous solution of 1 M $CuCl_2$ and 1 M HCl for 7 s).

deposition products, and due to the limited resolution depth of the EDS probe (top 2−10 microns). X-ray diffraction analysis (XRD) showed that the diffraction peaks of Cu became stronger with immersion time and suggested that the as-prepared Cu features were well-crystallized (Figure 1k). The copper diffraction peaks were located to the left of the peaks obtained for the as-received mesh constituents (0 s), and agreed well with standards (JCPDS Cards No. 03−1018 and 03−1209). The combined results of SEM, EDS and XRD confirm that metallic Cu formed on the surfaces of the stainless steel mesh wires after brief immersion, and that the leaf-like surface structures were indeed made of Cu metal. The formation of Cu microstructures on the meshes likely occurs through the simple chemical redox process[47]

$$Cu^{2+} + Fe \rightarrow Cu + Fe^{2+} \quad (1)$$

While the original stainless steel meshes appeared silvery white, the Cu-coated meshes appeared red (Figure 1l).

Figure 2a−c shows the variation of sessile contact angles (in air) of water, hexadecane, and chloroform (5 μL droplets) on stainless steel meshes immersed for specified periods in the $CuCl_2$−HCl solution and modified by subsequent exposure to stearic acid (STA), the second wet-processing step. The stainless meshes without STA modification [Figure 2a] were both super*hydrophilic* and super*oleophilic* when immersion times in the $CuCl_2$−HCl solution were greater than 2 s. Both water and oil droplets placed on the meshes spread completely onto the surface, giving contact angles of approximately 0°. Although the STA modification had no effect on the wettability by oil, the wettability by water was greatly affected. For a steel mesh immersed for 7 s in the $CuCl_2$−HCl solution, and subsequently 0.05 mol/L STA-modified for 20 min, the water contact and sliding angles [Figure 2b,c, respectively] were 160° ± 5.3° and 9° ± 2.3°, respectively, indicating a complete switch to superhydro*phobicity*, although super*oleophilicity* was retained [Figure 2b]. Treating the surface with STA is known to provide $-CH_3$ and $-CH_2-$ groups, which lowers the surface energy of the rough Cu structures,[48] thus making the mesh super-repellent to water. The simultaneous presence of super-hydrophobicity and superoleophilicity is critical for oil/water separation. To achieve this characteristic, STA modification is far more effective than a fluoropolymer (e.g., perfluorooctyl-triethoxysilane, FAS) coating, which makes the mesh oleophilic, thus causing the oil to spread too slowly for the separation to be effective (see Supporting Information, Video S1).

The influence of STA concentration and immersion time (in the STA solution) on wettability was also studied. The STA concentration was varied from 0.01 mol/L to 0.1 mol/L, and the immersion time was varied from 1 to 60 min, having a negligible influence on the water contact angles, as shown in Figure 3a. The sliding angles slightly increased with STA concentration, but the influence is small, as shown in Figure 3b. The immersion time variation from 1 to 60 min also had an almost negligible effect on sliding angles, meaning that the developed method induces high droplet mobility (sliding angle <10°) on roughened mesh substrates very quickly. In addition, the STA modification contributes to preserving the super-*hydrophobic*/super*oleophilic* behavior of the mesh for periods extending beyond several months (the advancing and receding angles shown in Figure 2b were measured after seven months, still showing very good superhydrophobicity). The super-hydrophobic meshes immersed for 7 s in the $CuCl_2$−HCl solution and subsequently modified with 0.05 mol/L STA exposure for 20 min were used as described in the following oil/water separation experiment.

To overcome the difficulty of existing oil/water separation methods, a new, simple, surface tension-driven, gravity-assisted approach and prototype filtering device to collect oil floating on

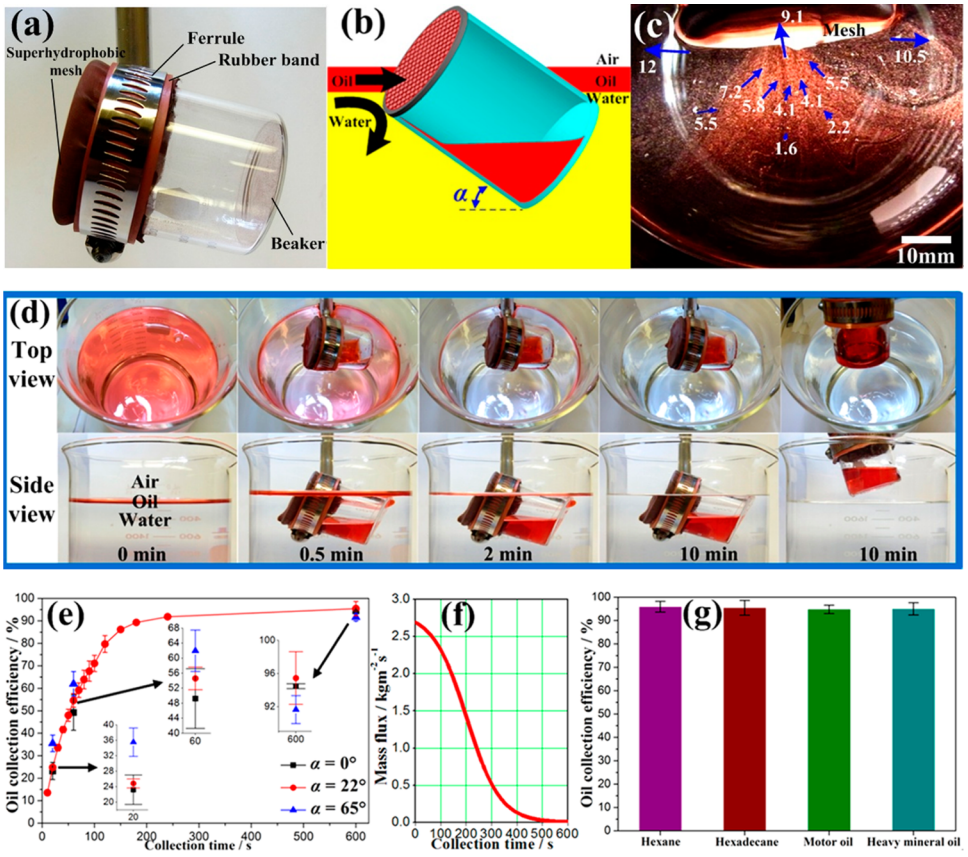

Figure 4. Surface-tension-driven, gravity-assisted oil/water separation and collection with superhydrophobic mesh-capped container. (a) Oil collection prototype device. (b) Schematic of the oil collection procedure. (c) Bulk motion of the oil film visualized by seeding the hexadecane with Cu nanoparticles and viewing from top (at 20 s collection, tilt angle $\alpha = 0°$, velocity vector magnitudes in mm/s). (d) Temporal stages of hexadecane oil collection, top and side views. (e) Hexadecane oil collection with time (collection rate is weakly sensitive to the tilt angle α of the container). (f) Temporal variation of oil (hexadecane) mass flux (mass flow rate per unit planform mesh area exposed to oil). (g) Oil collection efficiency of superhydrophobic mesh capped container for four oils with different kinematic viscosities.

water is described. The collection of floating oil using this method can occur in active flow conditions, such as those encountered with a slow-moving boat during oil-spill cleanup, or when a mesh-capped containment tank is anchored while floating in an ocean current. A small-scale oil collection prototype device is shown in Figure 4a, consisting of a superhydrophobic steel mesh mounted in a leak-proof manner on the open end of a 50 mL glass beaker that can be held in place at a variable angle α with respect to the horizontal. The beaker was partly immersed in a tilted fashion into a floating oil/water mixture (e.g., hexadecane/water) as shown in Figure 4b. Part of the mesh was submerged and remained in contact with both the floating oil and the water underneath. Because of the affinity of the oil toward the mesh, the floating hexadecane film wetted and spread over the mesh; the oil phase passed through the partly submerged mesh (which has negligible penetration resistance against the oil), flowed down along the inclined inner glass wall of the beaker, and collected by gravity at the bottom, while the water phase was not transmitted through the mesh and remained outside the collection vessel.

Interestingly, this mechanism created a bulk flow in the oil layer toward the mesh. Figure 4c shows a top-view snapshot of the bulk motion of the oil film in front of the mesh (at top of this image, held at $\alpha = 0°$) at 20 s after initiating the collection. The oil layer (seeded with microparticles for better visualization; velocity vectors were determined by tracking the moving particles over 200 ms) exhibits higher speeds closer to the mesh, while the entrained water (which could not penetrate the mesh) underneath the oil film is seen to turn outward parallel to the mesh as it becomes displaced by the oil flow into the mesh. This motion was sustained as long as an oil film existed on the water (see Supporting Information, Video S2). Similar oil bulk motion toward the mesh was observed when an isolated oil droplet (instead of a thick film) was dispensed at the upstream side of the mesh; the mesh drew in the droplet instantaneously (see Supporting Information, Video S3). This implies that the separation mechanism is effective not only for a continuous film-type spill, but also with discrete floating droplets or isolated oil volumes. Figure 4d shows an inclined ($\alpha = 22°$) beaker arrangement that allowed sustained oil/water separation until the floating oil in the pool was visibly depleted (the collecting beaker size was chosen large enough to hold the entire oil-phase contained in the original mixture).

The maximum pressure below which water could not penetrate the oil-infused superhydrophobic mesh was measured to be 1.58 ± 0.32 kPa (see Supporting Information, Section S1).[49] The water could not spread on the hexadecane-prewetted superhydrophobic mesh because of the negative spreading coefficient on this surface (see Supporting Information, Section S2). Further, water droplets placed on a horizontal oil-prewetted superhydrophobic mesh formed a hemispherical shape with a contact angle of 99.7 ± 1.5°. Water mobility on these surfaces was high, with a sliding angle as small as 6.1 ± 2.7°. These properties prevented the water from

entering the oil collection beaker, which then collected only the floating oil. The temporal variation of oil collection efficiency was quantified in terms of the oil collection coefficient R, defined as the instantaneous fractional oil collection

$$R(\%) = (M_c/M_o) \times 100\% \quad (2)$$

where M_0 and M_c denote the oil mass in the initial oil/water mixture and collected oil, respectively, at different collection times. Figure 4e shows that the oil collection efficiency rose steadily in the first 4 min and reached a near-saturation value (91.8 ± 0.85% of oil collected). After 10 min, almost 95.4 ± 3.2% of the oil had been collected from the surface of the water pool; at that time, the water surface appeared clean with minimal traces of floating oil [Figure 4d].

When examining the purity of the collected oil filtrate, the presence of water in the beaker-collected hexadecane was below the detection threshold (<0.9 wt %) of the DSC, thus indicating filtrate oil purity of 99 wt % or better. Because of the small uncertainty in the measurement technique (<0.9 wt %), there may or may not exist trace amounts of water in the oil filtrate below this detection threshold. Figure 4e further shows that the early oil collection rate slightly rose with tilting angle α because of the larger mesh area exposed to the oil layer at this orientation, likely due to the faster removal of the collected oil film formed at the back of the filtering mesh, which then travels down the sloped interior wall of the glass container.

In the above procedure, the superhydrophobic mesh-capped container *preferentially filtered and collected* the floating oil at the same time. Unlike the pouring-type method, this approach does not require collection of the oil/water mixture prior to separation but rather works with partial immersion of the mesh-equipped container into the oil-contaminated water, with the mesh exposed to both the oil and water phases. To quantify the oil collection ability of this method, the mass flux of oil (mass flow rate per unit planform mesh area exposed to oil) was measured, j_m, (see Supporting Information, Section S3 for detailed derivation). The temporal evolution of j_m is shown in Figure 4f. The separation process started with the highest mass intake rate (2.69 kg/m^{2}s), and after 4 min of collection, despite 91.8 ± 0.85% of oil having been collected, j_m remained as high as 1 kg/m^2 s. In addition, flux as a function of hydrostatic pressure was measured to better understand their relationship on a 7 s Cu- and 0.5 mol/L STA-treated mesh to optimize design parameters and operational ranges. For the three separate pressure values measured, 0.39, 0.78, and 1.57 kPa (or 4, 8, and 16 cm head using an in-house hydrostatic column with 1.1 cm inner dia.), the corresponding separation flux values for a 10 vol % water in hexadecane oil mixture were 2.22 ± 0.28, 3.71 ± 0.50, and 7.00 ± 0.66 kg/m^{2}s, respectively. The oil filtrate did not possess detectable levels of water even at the highest pressure tested, further strengthening the case for robust separation where no detectable traces of water were transmitted through the mesh filter.

The durability of the superhydrophobic mesh filter for repeated use was also examined. The performance of the as-prepared superhydrophobic mesh filter remained unchanged even after 58 complete separation cycles (see Supporting Information, Videos S4 and S5). SEM images confirmed that the oven-dried stainless steel mesh (290 °C for 20 min to remove residual hexadecane) remained covered with the Cu leaf microstructures [see Supporting Information, Figure S2a,b] after repeated use. EDS spectra showed that Cu and Fe remained on the mesh surfaces [see Supporting Information, Figure S2c], indicating that the rough Cu microstructures remain relatively unchanged after repetitive use.

In addition to hexadecane (kinematic viscosity 2.9 cSt at 40 °C), the method was found to be as effective in separating hexane (0.42 cSt at 40 °C) from water. It was also effective in separating motor oil (60.1 cSt at 40 °C) and heavy mineral oil (63.6−70.4 cSt at 40 °C) from water (see Supporting Information, Figure S3). All measured oil collection efficiencies for different oil types are shown in the bar graph of Figure 4g and were consistently better than 94%. The kinematic viscosities of light and medium crude oil at 40 °C are about 5.96 and 34.63 cSt, respectively, implying that this method should be as effective for real oil spills.[50,51] In practice, oil spill sites are often littered with other solid wastes/contaminants in the oil layer. Large solid debris can damage the rough Cu microstructures, thus degrading the oil collection efficiency of the mesh. This type of damage can be avoided by using an upstream grid with large pores that allow both water and oil through.

It is possible that smaller contaminants may, however, block the fine mesh pores and hinder oil recovery. To examine the robustness of the mesh filter in the presence of such fouling contaminants, PTFE particle powder was used (~1 μm diameter) to mimic microcontaminants and their effect on oil collection from hexadecane−PTFE dispersion/water mixtures. The oil collection velocity decreased due to the blockage caused by the PFTE powder reaching the mesh (see Supporting Information, Figure S4a), yet, 79.7% of the oil was still eventually collected after 90 min. The PFTE powder accumulated only on the mesh area exposed to oil [see Supporting Information, Figure S4b] leaving the other mesh areas clear of the particles and still effective for oil collection (see Supporting Information, Video S6). In this case, the PTFE particles were easily removed by a water jet, making the mesh capable of executing further separation cycles (see Supporting Information, Video S7). This is analogous to real-world defouling of contaminants on the mesh by ocean waves and/or fluid movement around the traveling mesh. A floating vessel could be equipped with side-mounted superhydrophobic mesh containment tanks [e.g., Supporting Information, Figure S5] making it possible for the collected oil to be continuously pumped/siphoned into the ship's hull, thus offering a high-rate collection method for the cleanup of large-area floating oil spills at sea.

It is important to note that both of the present superhydrophilic (non STA-treated) and superhydrophobic (STA-treated) meshes can also be used in the pouring-type, gravity-driven oil/water separation. Although there are many prior reports using this approach, none has consolidated the distinctly different conditions warranted for sustained separation of light oil/water vis-à-vis heavy oil/water mixtures. Considering this void in an otherwise pervasive reporting in this area, this issue is also addressed, demonstrating efficacy of these meshes for pouring-type separation as well. Generally, when using the pouring-type approach, the less dense liquid often contacted the mesh before the denser liquid. Once the denser liquid entered the separating container, it displaced the lower-density fluid and encountered the mesh. For this type of oil/water separation, only the superhydrophilic mesh that was prewetted with water could successfully and completely separate light oil and water (e.g., mixture of hexadecane and water); while for a heavy oil/water mixture (e.g., mixture of chloroform and water), either the superhydrophilic mesh that

was prewetted with oil or the dry superhydrophobic mesh provided sustained and complete separation (for details see Supporting Information, Section S4 and Videos S8–S13).

4. CONCLUSIONS

A facile method to fabricate large-area, selective-wettability (superhydrophobic and superoleophilic) stainless steel mesh has been demonstrated. The superhydrophobic mesh offers the foundation for operating a novel surface-tension-driven, gravity-assisted, floating-oil collection prototype device consisting of a container capped with this mesh, as demonstrated and analyzed. The device circumvents the drawbacks of traditional oil absorbent and oil/water filtration materials in the pouring-type, gravity-driven method, by simultaneously filtering and collecting floating oil from oil–water mixtures. The present approach achieves excellent oil collection efficiencies (>94%) and high filtrate purities (>99 wt %) for oils with wide-ranging kinematic viscosities (0.32–70.4 cSt at 40 °C), including motor oil and heavy mineral oil. The prototype device showed high stability and functionality over repeated use, and has scale-up prospects for efficient cleanup of large oil spills on seawater. If one considers a floating vessel equipped with such a device, the performance metrics described in this study suggest that oil collection can occur at mesh submersion depths of less than 1 m and vessel floating speeds of a few m/s; these values make the present approach attractive for large-scale oil spill cleanup. Moreover, the measured oil collection rates changed only slightly over a wide range of container tilting angles, thus offering assurances of reliable operation in the field (e.g., in rough seas) where the tilt angle may vary due to the movement of the vessel or the presence of waves. Finally, the continued operation of the device, albeit with reduced effectiveness, in the presence of solid particle contaminants exemplifies the flexibility and robustness of the technique. Additionally, using a superhydrophilic mesh, a consolidation of various separation techniques was demonstrated for gravity-driven, pouring-type separation of oil/water mixtures so that various approaches reported in the literature could be reconciled.

■ ASSOCIATED CONTENT

Supporting Information

Resistance to water penetration through the oil-infused superhydrophobic mesh, spreading coefficient of water on the oil-infused superhydrophobic mesh, oil mass collection flux, detailed analysis of pouring-type gravity-driven oil/water separation, surface morphology and chemical composition of superhydrophobic mesh after 58 complete separation cycles, separation and collection of oil from motor oil/water mixture and hexadecane-PTFE particle mixture floating on water, schematic of a large-scale skimmer vessel, schematic depiction and experimental images of wetting behavior of oil droplets under water, and water droplets under oil on different meshes, pouring-type gravity-driven oil/water separation using different types of wettability-modified steel meshes, and videos of separation processes. This material is available free of charge via the Internet at http://pubs.acs.org.

■ AUTHOR INFORMATION

Corresponding Authors

*E-mail: cmm@uic.edu. Phone: +1 312 996 3436. (C.M.M.)
*E-mail: wenjixu@dlut.edu.cn. Phone: +86 4118470 8422. (W.X.)

Notes

The authors declare no competing financial interest.

■ ACKNOWLEDGMENTS

The authors are grateful for financial support from National Natural Science Foundation of China (NSFC, Grant No. 90923022).

■ REFERENCES

(1) Zhu, S.; Strunin, D. A. Numerical Model for the Confinement of Oil Spill with Floating Booms. *Spill Sci. Technol. Bull.* **2002**, *7*, 249–255.
(2) Bayat, A.; Aghamiri, S. F.; Moheb, A.; Vakili-Nezhaad, G. R. Oil Spill Cleanup from Sea Water by Sorbent Materials. *Chem. Eng. Technol.* **2005**, *28*, 1525–1528.
(3) Adebajo, M. O.; Frost, R. L.; Kloprogge, J. T.; Carmody, O.; Kokot, S. Porous Materials for Oil Spill Cleanup: A Review of Synthesis and Absorbing Properties. *J. Porous Mater.* **2003**, *10*, 159–170.
(4) Radetić, M. M.; Jocić, D. M.; Jovančić, P. M.; Petrović, Z. L.; Thomas, H. F. Recycled Wool-Based Nonwoven Material as an Oil Sorbent. *Environ. Sci. Technol.* **2003**, *37*, 1008–1012.
(5) Zhu, Q.; Pan, Q.; Liu, F. Facile Removal and Collection of Oils from Water Surfaces through Superhydrophobic and Superoleophilic Sponges. *J. Phys. Chem. C* **2011**, *115*, 17464–17470.
(6) Lessard, R. R.; DeMarco, G. The Significance of Oil Spill Dispersants. *Spill Sci. Technol. Bull.* **2000**, *6*, 59–68.
(7) Atlas, R. M. Petroleum Biodegradation and Oil Spill Bioremediation. *Mar. Pollut. Bull.* **1995**, *31*, 178–182.
(8) Li, K.; Ju, J.; Xue, Z.; Ma, J.; Feng, L.; Gao, S.; Jiang, L. Structured Cone Arrays for Continuous and Effective Collection of Micron-Sized Oil Droplets from Water. *Nat. Commun.* **2013**, *4*, 1.
(9) Xue, Z.; Cao, Y.; Liu, N.; Feng, L.; Jiang, L. Special Wettable Materials for Oil/Water Separation. *J. Mater. Chem. A* **2014**, *2*, 2445.
(10) Tuteja, A.; Choi, W.; Ma, M. L.; Mabry, J. M.; Mazzella, S. A.; Rutledge, G. C.; McKinley, G. H.; Cohen, R. E. *Science* **2007**, *318*, 1618–1622.
(11) Deng, X.; Mammen, L.; Butt, H.; Vollmer, D. Candle Soot as a Template for a Transparent Robust Superamphiphobic Coating. *Science* **2012**, *335*, 67–70.
(12) Bhushan, B.; Jung, Y. C. Natural and Biomimetic Artificial Surfaces for Superhydrophobicity, Self-Cleaning, Low Adhesion, and Drag Reduction. *Prog. Mater. Sci.* **2011**, *56*, 1–108.
(13) Feng, L.; Li, S.; Li, Y.; Li, H.; Zhang, L.; Zhai, J.; Song, Y.; Liu, B.; Jiang, L.; Zhu, D. Super-Hydrophobic Surfaces: From Natural to Artificial. *Adv. Mater.* **2002**, *14*, 1857–1860.
(14) Liu, K.; Tian, Y.; Jiang, L. Bio-Inspired Superoleophobic and Smart Materials: Design, Fabrication, and Application. *Prog. Mater. Sci.* **2013**, *58*, 503–564.
(15) Darmanin, T.; de Givenchy, E. T.; Amigoni, S.; Guittard, F. Superhydrophobic Surfaces by Electrochemical Processes. *Adv. Mater.* **2013**, *25*, 1378–1394.
(16) Wu, J.; Wang, N.; Wang, L.; Dong, H.; Zhao, Y.; Jiang, L. Electrospun Porous Structure Fibrous Film with High Oil Adsorption Capacity. *ACS Appl. Mater. Interfaces* **2012**, *4*, 3207–3212.
(17) Lin, J.; Ding, B.; Yang, J.; Yu, J.; Sun, G. Subtle Regulation of the Micro- and Nanostructures of Electrospun Polystyrene Fibers and Their Application in Oil Absorption. *Nanoscale* **2012**, *4*, 176–182.
(18) Zhu, H.; Qiu, S.; Jiang, W.; Wu, D.; Zhang, C. Evaluation of Electrospun Polyvinyl Chloride/Polystyrene Fibers As Sorbent Materials for Oil Spill Cleanup. *Environ. Sci. Technol.* **2011**, *45*, 4527–4531.
(19) Lin, J.; Tian, F.; Shang, Y.; Wang, F.; Ding, B.; Yu, J. Facile Control of Intra-Fiber Porosity and Inter-Fiber Voids in Electrospun Fibers for Selective Adsorption. *Nanoscale* **2012**, *4*, 5316–5320.
(20) Chen, N.; Pan, Q. Versatile Fabrication of Ultralight Magnetic Foams and Application for Oil–Water Separation. *ACS Nano* **2013**, *7*, 6875–6883.

(21) Zhu, Q.; Chu, Y.; Wang, Z.; Chen, N.; Lin, L.; Liu, F.; Pan, Q. Robust Superhydrophobic Polyurethane Sponge as a Highly Reusable Oil-Absorption Material. *J. Mater. Chem. A* **2013**, *1*, 5386−5393.
(22) Nagappan, S.; Park, J. J.; Park, S. S.; Lee, W.; Ha, C. Bio-Inspired, Multi-Purpose and Instant Superhydrophobic-Superoleophilic Lotus Leaf Powder Hybrid Micro-Nanocomposites for Selective Oil Spill Capture. *J. Mater. Chem. A* **2013**, *1*, 6761−6769.
(23) Calcagnile, P.; Fragouli, D.; Bayer, I. S.; Anyfantis, G. C.; Martiradonna, L.; Cozzoli, P. D.; Cingolani, R.; Athanassiou, A. Magnetically Driven Floating Foams for the Removal of Oil Contaminants from Water. *ACS Nano* **2012**, *6*, 5413−5419.
(24) Cheng, M.; Ju, G.; Jiang, C.; Zhang, Y.; Shi, F. Magnetically Directed Clean-up of Underwater Oil Spills through A Functionally Integrated Device. *J. Mater. Chem. A* **2013**, *1*, 13411−13416.
(25) Cheng, M.; Gao, Y.; Guo, X.; Shi, Z.; Chen, J.; Shi, F. A Functionally Integrated Device for Effective and Facile Oil Spill Cleanup. *Langmuir* **2011**, *27*, 7371−7375.
(26) Wang, S.; Li, M.; Lu, Q. Filter Paper with Selective Absorption and Separation of Liquids that Differ in Surface Tension. *ACS Appl. Mater. Interfaces* **2010**, *2*, 677−683.
(27) Gui, X.; Zeng, Z.; Lin, Z.; Gan, Q.; Xiang, R.; Zhu, Y.; Cao, A.; Tang, Z. Magnetic and Highly Recyclable Macroporous Carbon Nanotubes for Spilled Oil Sorption and Separation. *ACS Appl. Mater. Interfaces* **2013**, *5*, 5845−5850.
(28) Cervin, N.; Aulin, C.; Larsson, P.; Wågberg, L. Ultra Porous Nanocellulose Aerogels as Separation Medium for Mixtures of Oil/Water Liquids. *Cellulose* **2012**, *19*, 401−410.
(29) Tang, Y.; Yeo, K. L.; Chen, Y.; Yap, L. W.; Xiong, W.; Cheng, W. Ultralow-Density Copper Nanowire Aerogel Monoliths with Tunable Mechanical and Electrical Properties. *J. Mater. Chem. A* **2013**, *1*, 6723−6726.
(30) Hayase, G.; Kanamori, K.; Fukuchi, M.; Kaji, H.; Nakanishi, K. Facile Synthesis of Marshmallow-like Macroporous Gels Usable under Harsh Conditions for the Separation of Oil and Water. *Angew. Chem., Int. Ed.* **2013**, *52*, 1986−1989.
(31) Feng, L.; Zhang, Z.; Mai, Z.; Ma, Y.; Liu, B.; Jiang, L.; Zhu, D. A Super-Hydrophobic and Super-Oleophilic Coating Mesh Film for the Separation of Oil and Water. *Angew. Chem., Int. Ed.* **2004**, *43*, 2012−2014.
(32) Kota, A. K.; Kwon, G.; Choi, W.; Mabry, J. M.; Tuteja, A. Hygro-Responsive Membranes for Effective Oil−Water Separation. *Nat. Commun.* **2012**, *3*, 1025.
(33) Xue, Z.; Wang, S.; Lin, L.; Chen, L.; Liu, M.; Feng, L.; Jiang, L. A Novel Superhydrophilic and Underwater Superoleophobic Hydrogel-Coated Mesh for Oil/Water Separation. *Adv. Mater.* **2011**, *23*, 4270−4273.
(34) Gao, C.; Sun, Z.; Li, K.; Chen, Y.; Cao, Y.; Zhang, S.; Feng, L. Integrated Oil Separation and Water Purification by A Double-Layer TiO_2-Based Mesh. *Energy Environ. Sci.* **2013**, *6*, 1147−1151.
(35) Zhang, F.; Zhang, W. B.; Shi, Z.; Wang, D.; Jin, J.; Jiang, L. Nanowire-Haired Inorganic Membranes with Superhydrophilicity and Underwater Ultralow Adhesive Superoleophobicity for High-Efficiency Oil/Water Separation. *Adv. Mater.* **2013**, *25*, 4192−4198.
(36) Zhang, L.; Zhong, Y.; Cha, D.; Wang, P. A Self-Cleaning Underwater Superoleophobic Mesh for Oil-Water Separation. *Sci. Rep.* **2013**, *3*, 1.
(37) Zhou, X.; Zhang, Z.; Xu, X.; Guo, F.; Zhu, X.; Men, X.; Ge, B. Robust and Durable Superhydrophobic Cotton Fabrics for Oil/Water Separation. *ACS Appl. Mater. Interfaces* **2013**, *5*, 7208−7214.
(38) Wang, B.; Guo, Z. Superhydrophobic Copper Mesh Films with Rapid Oil/Water Separation Properties by Electrochemical Deposition Inspired from Butterfly Wing. *Appl. Phys. Lett.* **2013**, *103*, 063704.
(39) Liang, J.; Zhou, Y.; Jiang, G.; Wang, R.; Wang, X.; Hu, R.; Xi, X. Transformation of Hydrophilic Cotton Fabrics into Superhydrophobic Surfaces for Oil/Water Separation. *J. Text. Inst.* **2013**, *104*, 305−311.
(40) Jing, B.; Wang, H.; Lin, K.; McGinn, P. J.; Na, C.; Zhu, Y. A Facile Method to Functionalize Engineering Solid Membrane Supports for Rapid and Efficient Oil−Water Separation. *Polymer* **2013**, *54*, 5771−5778.
(41) Yang, H.; Zhang, X.; Cai, Z.; Pi, P.; Zheng, D.; Wen, X.; Cheng, J.; Yang, Z. Functional Silica Film on Stainless Steel Mesh with Tunable Wettability. *Surf. Coat. Technol.* **2011**, *205*, 5387−5393.
(42) Wen, Q.; Di, J.; Jiang, L.; Yu, J.; Xu, R. Zeolite-Coated Mesh Film for Efficient Oil-Water Separation. *Chem. Sci.* **2013**, *4*, 591−595.
(43) Tian, D.; Zhang, X.; Tian, Y.; Wu, Y.; Wang, X.; Zhai, J.; Jiang, L. Photo-Induced Water-Oil Separation Based on Switchable Superhydrophobicity-Superhydrophilicity and Underwater Superoleophobicity of The Aligned ZnO Nanorod Array-Coated Mesh Films. *J. Mater. Chem.* **2012**, *22*, 19652−19657.
(44) Li, H.; Zheng, M.; Ma, L.; Zhu, C.; Lu, S. Two-Dimensional ZnO Nanoflakes Coated Mesh for The Separation of Water and Oil. *Mater. Res. Bull.* **2013**, *48*, 25−29.
(45) Wang, F.; Lei, S.; Xue, M.; Ou, J.; Li, W. In Situ Separation and Collection of Oil from Water Surface via a Novel Superoleophilic and Superhydrophobic Oil Containment Boom. *Langmuir* **2014**, *30*, 1281−1289.
(46) Liu, N.; Chen, Y.; Lu, F.; Cao, Y.; Xue, Z.; Li, K.; Feng, L.; Wei, Y. Straightforward Oxidation of a Copper Substrate Produces an Underwater Superoleophobic Mesh for Oil/Water Separation. *ChemPhysChem* **2013**, *14*, 3489−3494.
(47) Bu, X. W. *Fabrication and Applied Research of Superhydrophobic and Superoleophilic Strainer Mesh;* Dalian University of Technology: Dalian, China, 2014.
(48) Song, J.; Lu, Y.; Huang, S.; Liu, X.; Wu, L.; Xu, W. A Simple Immersion Approach for Fabricating Superhydrophobic Mg Alloy Surfaces. *Appl. Surf. Sci.* **2013**, *266*, 445−450.
(49) Liu, N.; Cao, Y. Z.; Lin, X.; Chen, Y. N.; Feng, L.; Wei, Y. A Facile Solvent-Manipulated Mesh for Reversible Oil/Water Separation. *ACS Appl. Mater. Interfaces* **2014**, *6*, 12821−12826.
(50) Harvey, E. H. The Surface Tension of Crude Oils. *Ind. Eng. Chem.* **1925**, *17*, 85.
(51) Al-Besharah, J. M.; Salman, O. A.; Akashah, S. A. Viscosity of Crude Oil Blends. *Ind. Eng. Chem. Res.* **1987**, *26*, 2445−2449.